



# The Combined System of Microlensing Exoplanets and Their Host Stars

# 79

Uffe Gråe Jørgensen and Markus Hundertmark

## Contents

Introduction . . . . .	1642
The Basic Principle . . . . .	1643
The Statistical Significance of Even Few Planet Detections . . . . .	1644
The Advantage of Simultaneous Ground- and Space-Based Observations . . . . .	1645
Revealing Small-Mass Exoplanets, Smaller Stars, and Free-Floating Planets . . . . .	1648
The Source Star Atmosphere . . . . .	1650
Summary . . . . .	1651
References . . . . .	1653

## Abstract

If the direction to a foreground star (the lens) and a background star (the source) is aligned to within approximately a milli-arc second (mas), then the foreground star will redirect light from the background star, thereby increasing its apparent brightness, forming a microlensing event. The light curve, i.e., the increase in source brightness as function of time, mainly contain information about the lens star and its exoplanets, but higher order details also depend on the source star and its possible exoplanets, so the most detailed analyses require simultaneous model fit to all the components. The models can reveal the mass and dynamics of the system but can also reveal details of, for example, the atmospheric structure of the

U. G. Jørgensen (✉)

Centre for Star and Planet Formation, Niels Bohr Institute, University of Copenhagen, Copenhagen, Denmark

e-mail: [uffegj@nbi.ku.dk](mailto:uffegj@nbi.ku.dk)

M. Hundertmark

Astronomisches Rechen-Institut, Zentrum für Astronomie der Universität Heidelberg (ZAH), Heidelberg, Germany

e-mail: [markus.hundertmark@uni-heidelberg.de](mailto:markus.hundertmark@uni-heidelberg.de)

source star. Microlensing is an optimal method to obtain unbiased information about the stellar lens population, detailed information about the source star atmosphere, and statistics on exoplanets with mass and orbits similar to the planets in the solar system, including planets beyond the snow line and even unbound planets. Microlensing events can be found in a wide distance range throughout our own Galaxy, as well as in principle in other galaxies too.

---

## Introduction

For the bulk of all known exoplanets, no one has ever seen the planet itself but only its effect on its host star or another object. Microlensing is extreme in this respect, because usually not even the host star (i.e., the lensing star) is visible. The lensing system is usually a few kpc in front of the visible source, which is itself most often a giant star near the Galactic center. At first glance one could be tempted to think that this lack of access to direct observations of the lensing star and its planets was a drawback compared to other methods, but it has some remarkable advantages too, among them that the (lensing) host stars are chosen at random by nature itself, independent of the observer, and therefore are unaffected by the observational biases that haunt most other exoplanet search methods. This assures the microlensing observations a very high and well-understood statistical value, both concerning the exoplanets and their host stars. The lensing objects are a simple function of their relative abundance in nature, and they include unbound planets, brown dwarfs, white dwarfs, neutron stars, and black holes, because the method is independent of light from the lens, only on its mass.

In addition, the microlensing method is complementary to the transit and radial velocity methods in the parameter space it covers, with its main sensitivity being to planets resembling those in our own solar system, including planets beyond the snow line. The planetary mass range that has been reached, with present-day technology, spans from slightly above one Earth mass to the brown dwarf limit and beyond, in orbits ranging from inside that of Mercury out to that of Neptune, and with a future potential to reach considerably smaller planets as well as the population of unbound (i.e., free floating) planets (Mróz et al. 2017). So far, only exoplanets orbiting lens stars have been identified, and lensing exoplanets have been discovered anywhere between a few hundred pc (parsec) from us and all the way to the Galactic center itself, but typical lenses are a few kpc (1 kpc = 1000 pc) away. With more accurate and advanced observing (e.g., Mackay et al. 2017) and more complex modeling (e.g., Bennett et al. 2018), it will in the future most likely be possible to extract information about the source star exoplanetary systems too.

Finally, the microlensing method is not limited to nearby stars. The type of questions that can be answered with statistical confidence from microlensing observations therefore includes “which type of stars have which type of planetary systems?”, “how abundant are planetary systems similar to our own?”, “do different regions of our Galaxy harbor different types of planetary systems?”, “how is the

abundance of planets related to stellar populations?”, and even questions like “do the nearest galaxies have the same trends in stars and their planetary systems as our own Galaxy?”.

## The Basic Principle

In the simplest approximation, when the lens and the source are considered point sources, and the Earth is considered non-moving during the event, the light from the source star will increase and decrease again symmetrically in time, while the angular distance  $u(t)$  between the line of sight to the lens and the source approach each other and depart again during their, and our, relative movements in the Galaxy. It was this simple approximation Einstein used in his first prediction of the phenomenon (Einstein 1936, elaborated further by Refsdal 1964, and others), where he calculated that the magnification,  $A(t)$ , of the source star due to the lens passage was a function of  $u(t)$  only:

$$A(t) = \frac{u(t)^2 + 2}{u(t)\sqrt{u(t)^2 + 4}} \quad (1)$$

The function  $A = A(t)$  is called the microlensing light curve, and in its simple form of Eq. 1 often also called a Paczynski curve. The *possibility* of observing a source star being lensed (i.e., the amount of amplification necessary in order to detect it with a given instrument) is therefore, in this approximation, independent of the mass of the lensing object. The *probability* of discovering the event is, however, dependent on the mass of the lensing object, because the angular distance, the so-called Einstein radius  $\Theta_E$ , from the lensing object which the source star has to pass within in order to be magnified, is proportional to the square root of the mass,  $M_L$ , of the lensing object:

$$\Theta_E = \sqrt{\frac{4GM_L}{c^2} \frac{D_{LS}}{D_L D_S}} = \tilde{k} \sqrt{M_L} \sqrt{\frac{D_{LS}}{D_L D_S}} \quad (2)$$

where  $D_{LS}$  is the distance between the lens and the source,  $D_L$  the distance between the lens and the observer, and  $D_S$  the distance between the source and the observer. If  $M_L$  is expressed in units of  $M_\odot$ , and  $D_L$ ,  $D_S$ , and  $D_{LS}$  in kpc, then  $\tilde{k}=2.85$  will give  $\Theta_E$  in mas (milli-arc seconds).

Equation 2 enters Eq. 1 because  $u(t)$  is in units of  $\Theta_E$ , and we see from Eq. 1 that when the angular distance between the source and the lens is  $\Theta_E$ , then  $A(t) = 3/\sqrt{5} = 1.34$ . It is therefore easy to localize when the angular distance between the source and the lens is  $\Theta_E$  (i.e.,  $u(t) = 1$  or  $A(t)=1.34$ ), and since the top,  $A(t_0)$ , of the light curve is also easily measurable, the minimum distance  $u(t_0)$  of the passage is known from Eq. 1, and hence it can be calculated from the light curve how long time,  $t_E$ , it takes the source star to pass one  $\Theta_E$ .

If the relative angular speed, the proper motion  $\mu$ , of the source and the lens is known (or estimated from a Galactic model), then  $\Theta_E$  can be calculated from

$$\Theta_E = t_E \mu \quad (3)$$

Most often the source star will be a giant close to the Galactic center, i.e., at  $D_S = 8$  kpc, just simply because the density of stars increases rapidly toward the Galactic center, such that most of the bright stars seen in the direction of the Galactic center actually also physically are in or near to the center. If also  $D_L$  is known (see later), then the mass,  $M_L$ , of the lensing star can now be calculated from a simple observation of the light curve and using just Eqs. 1, 2, and 3.

---

## The Statistical Significance of Even Few Planet Detections

In praxis it can often be difficult to estimate well some of the parameters  $\mu$ ,  $D_L$ , and  $D_S$ , but the important message at this stage, in understanding something about the host stars of microlensing exoplanets, is that all types of lens stars can give rise to equally large amplifications of the light from the source stars (and hence be equally easy to observe). Detection of a lens star (and its planets) is not dependent on being able to see the light from the lens, but only on the relative geometrical configuration of the source and the lens, and our ability to see the magnified source. The probability of a lens star at a given distance  $D_L$  amplifying the light from a given background star at distance  $D_S$  is therefore a well-determined function of its mass  $M_L$ , calculable through Eqs. 1 and 2. Hence, the host star mass distribution function, eventually for various types of exoplanets, can be readily calculated from a sample of microlensing observations. Likewise, the probability of detecting exoplanets of given mass and orbital parameters to a given mass host star is a well-determined function. As a consequence, relatively few microlensing exoplanets can have high statistical significance compared to even a much larger number of exoplanets discovered by other methods. Detailed statistical analyses of microlensing exoplanets have already been successfully performed based on the relatively modest number of microlensing exoplanets known today, giving important and solid statistics on the distribution of giant planets beyond the snow line (Gould et al. 2010), the planetary mass distribution function in the terrestrial regime (Cassan et al. 2012), the mass distribution function for very low-mass exoplanets (Udalski et al. 2018), as well as the ratio between planets and brown dwarf companions orbiting low-mass stars (Shvartzvald et al. 2016a). Hence also the statistics of planet types as function of stellar type (mass) and distance in the Galaxy can be computed directly from Eqs. 1 and 2 once sufficient numbers of microlensing planets are known. Microlensing is the only known method that allow such statistical analysis over large distances in our Galaxy and beyond to the nearest other galaxies (Ingrasso et al. 2009) and potentially even to far away galaxies too (Dai and Guerras 2018).

When exoplanetary microlensing was first discussed around 1990 (e.g., Mao and Paczynski 1991; Gould and Loeb 1992) and for many years to follow, most

people envisioned that the method would only be able to contribute with the relative planetary to host star mass and the instantaneous orbital projected distance between the star and planet relative to the lensing distance from us. However, with the ability today to include higher-order effects from the theory into fast computer codes, and by the help of much more advanced observational techniques than originally envisioned, determination of the absolute mass of the host star is today possible, together with the physical dimensions of the source star and detailed orbital parameters of the planets orbiting the lensing star, such as orbital eccentricity and inclination (Gaudi et al. 2008; Ryu et al. 2018). In principle the same set of information could be deduced for the source star, although no source star planets have yet been confirmed.

---

### The Advantage of Simultaneous Ground- and Space-Based Observations

On the observational side, an important breakthrough was reached when it became possible to make simultaneous observations from the ground and from satellite, first with Rosetta, and later more systematically by use of Kepler, Spitzer, and Swift (Yee et al. 2015; Henderson et al. 2016; Shvartzvald et al. 2016b; Ryu et al. 2018), and in the future perhaps by use of WFIRST, Euclid, and/or a dedicated microlensing satellite. If a satellite is at a projected distance  $D_{\perp}$  from Earth during a lensing event, the distance to the lens can be determined from the parallax, together with the relative angular velocity  $\mu$  of the lens and source, by noting that the difference in time,  $\Delta t$ , of the maximum of the light curve as seen from Earth and from the satellite is given (from simple geometry) as

$$\Delta t = D_{\perp} / (tg(\mu) \times D_L) \quad (4)$$

If  $D_{\perp}$  is 1.2 AU,  $\mu=0.4$  mas/month,  $D_L=3.3$  kpc, and  $D_S=8$  kpc, then  $\Delta t$  would be approximately 3 weeks, which show us that typical values of involved distances and relative angular speeds will give us a shift of a few weeks of a light curve seen from a satellite in Spitzer's orbit compared to observations from the ground. With such distances and time scales, quite accurate estimates of  $D_L$  and  $\mu$  can be given from the observations, and hence also the absolute mass of the lensing star and the relative movements of the lens and source could be estimated just from Eqs. 1, 2, and 3.

In praxis of course more details in the geometry, movement, and higher-order effects will be included in a real analysis of the observations, but the above equations illustrate the principle, and the numbers given in the example correspond well to the case of the Neptune-mass exoplanet OGLE-2015-BLG-0966Lb in a 2.3 AU orbit around a  $0.38M_{\odot}$  M dwarf 3.3 kpc from us in the direction of the Galactic center. The combined ground and Spitzer observations of this particular object were described by Street et al. (2016) where also the more detailed explanation and analysis can be found. The main message is that quite accurate values of the mass, distance, and movement of individual stars (with or without planets) can be

determined from microlensing when combined ground and satellite observations are available.

If the lensing object is not a point-like single object (such as a single main sequence star or a compact stellar remnant), then the analysis most often cannot even qualitatively be described by the simple formulas above. Such a multiple lens system could be a binary star or a star orbited by one or more planets. The Einstein ring is then substituted by a so-called critical curve. In the case of a planet far from the star, the critical curve around the star looks quite similar to the single-star Einstein ring, with an additional ring structure around the planetary position, with the radius of the two reflecting their mass ratio according to Eq. 2. In the case of a planet on or inside the stellar Einstein ring, the combined stellar-planetary critical curve looks somewhat deformed. The major difference between the single and multiple lens, however, is the substitution of the central point where the magnification is infinite in the single point-source-point-lens case with a number of so-called caustic curves where the magnification formally is also infinite (in the point-source approximation). The caustic curves form closed figures, the individual caustic lines are called folds, and the regions where two folds meet are called cusps. The magnification pattern (i.e., the light curve) depends critically on the caustic topology and the movement of the source through it. An analysis of a binary lens will therefore usually involve a detailed Monte Carlo simulation where different configurations and movements are simulated. The best fit to the observed light curve is therefore a simultaneous best estimate of both the planetary and the host star parameters.

Today, the observational data are usually uploaded online to a server that performs the best fit light curve analysis online and automatically alert the community about potential deviations in the light curve that could be due to the effects of an orbiting exoplanet. Such analysis is, for example, done by the MiNDSTeP team by use of the SIGNALMEN software package (Dominik et al. 2007) and further analyzed online to the prediction of various host star exoplanetary configurations and their likelihood by use of the method described in Bozza (2012). The software now includes the observations from most teams worldwide and can be followed online on [www.mindstep-science.org](http://www.mindstep-science.org).

In the case of OGLE-2015-BLG-0966, the exoplanetary deviation from the stellar light curve lasted 6 h (see Fig. 1), and a simple scaling of Eq. 2 would have given us  $M_{\text{pl}} = 10 M_{\oplus}$ , only a factor 2 from the real value of  $21 M_{\oplus}$  reached by a more detailed and simultaneous solution of the best fit stellar and planetary parameters. This, however, is only a coincidence caused by the fact that the source star passed just outside the central cusp (as seen in Fig. 1) and in this way experienced a planetary magnification pattern not very different from what would have been caused if the source had passed through a corresponding separated Einstein ring of a planet in a wide orbit (but in that case the planetary deviation would not have been close to the maximum of the stellar magnification pattern). In general the planetary deviation can be a magnification as well as a demagnification compared to the stellar light curve, depending on the details of the caustic topology and the source star's movement through it or close to it.

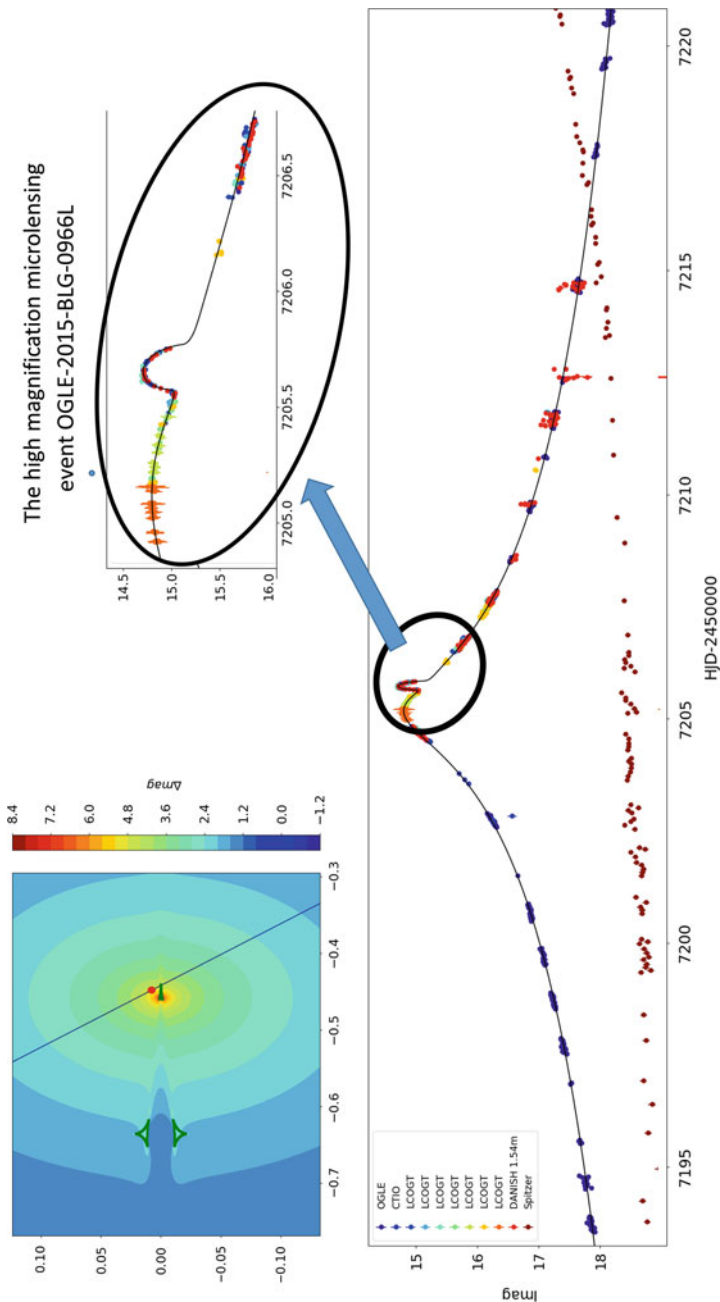


**Fig. 1** A high-magnification lensing event observed in 2015 simultaneously from the ground and from the Spitzer space telescope. The lower panel shows the light curve observed by several observatories from the ground (many colors with fitted line) and from space (brown points) during the 4 weeks from HJD 7193 to 7221. Note the large space parallax shift of  $\approx 3$  weeks of the light curves seen from ground and from Spitzer. The clear planetary deviation at HJD day  $\approx 7206$  (near the top, seen best in the upper right inset) reveals a planet of  $21 M_{\oplus}$  in an orbit of semimajor axis 2.3 AU. The upper left panel shows the planetary caustics (dark green lines), the magnification regions (color scale), and the computed best fit source path

In principle parallax estimates as in Fig. 1 could be obtained from combining observations at different locations on Earth instead (e.g., Gould et al. 2009), but the accuracy is better if the distance between the observation sites is as big as between Earth and a satellite at large distances, such as Spitzer or Rosetta. Large distances between the observing points can also be obtained if the event lasts long enough time, since the different viewing points from Earth being in different positions of its orbit then can be used. This was the case for the rather complex event OGLE-2006-BLG-109 shown in Fig. 2 (Gaudi et al. 2008). A fortunate passage of the source star through the caustic regions caused by two different giant planets made the caustic passages span 12 full days, enough for the Earth to have moved a substantial fraction of an AU and therefore for the different viewing angles to the caustics to be taken into account in the modeling. As a result it was possible to include more orbital parameters into the solution than is most often the case. A similarly fortunate case was observed for OGLE-2016-BLG-1190Lb observed simultaneously from ground and from Spitzer (Ryu et al. 2018).

Although the basic theory of microlensing goes back to 1936, its full application is still in its infancy, and many less frequent possibilities have not yet been explored in praxis. This goes, for example, for the possibility of seeing debris disks around the lensing stars (Hundertmark et al. 2009) or the effect of circumstellar disks around the source stars (Sajadian and Rahvar 2015). Also, the whole area of astrometric microlensing is still to be observationally explored, even though the theory has been described already since a few decades ago (Høg et al. 1995; Paczynski 1998).

---

## Revealing Small-Mass Exoplanets, Smaller Stars, and Free-Floating Planets

The reason why  $A(t)$  in Eq. 1 does not in reality become infinity when  $u(t)$  goes toward zero is that Eq. 1 only is valid for point sources, i.e., when the angular radius,  $\Theta_S$ , of the source star goes toward zero. The smaller (i.e., the more “point-like”) the source star is, the stronger and shorter the magnification will be. A large source star will smear out the deviation – the different regions of the source star are not amplified to maximum at the same time. Integrating over the surface of the source star shows that  $A(t)$  can only reach a maximum amplification:

$$A_{\max} = \sqrt{1 + 4(\Theta_E/\Theta_S)^2} \quad (5)$$

Since  $(\Theta_E)^2 \propto M_L$  and  $(\Theta_S)^2 \propto L_S$  (the source star luminosity), then a low-mass host star or brown dwarf population is best identified by observing small source stars, and in particular small-mass exoplanets are best observed by identifying small source stars in the field. Ten times smaller-mass planets require identifying ten times less luminous background stars, and in crowded fields the identification of low luminosity stars is determined by the spatial resolution of the images, not by the exposure time or the size of the telescope. Improved resolution can be obtained by



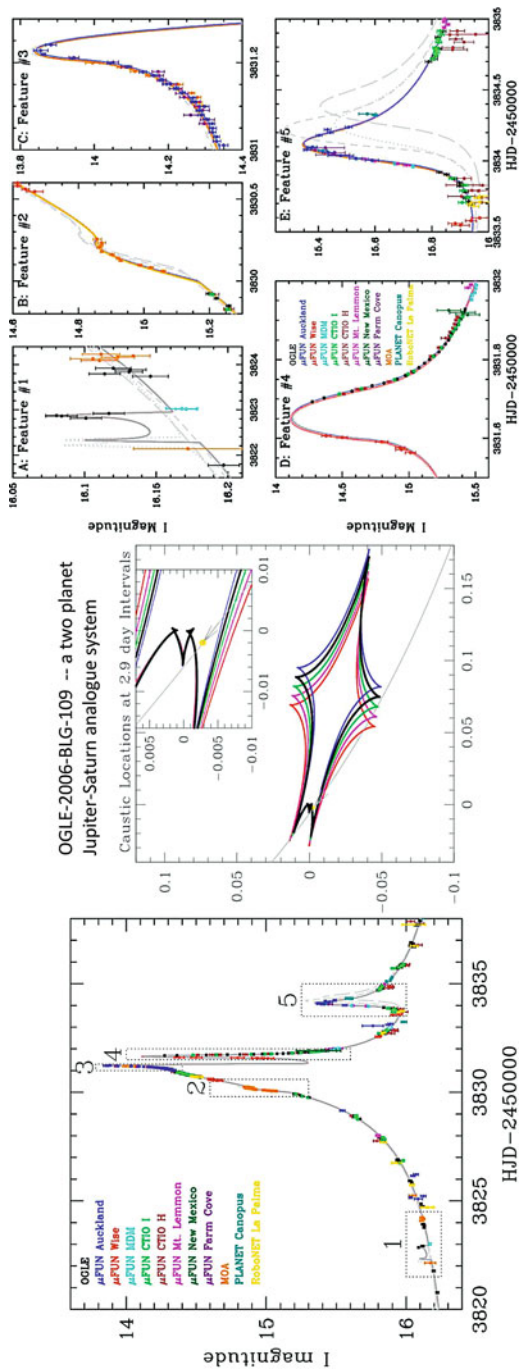


**Fig. 2** OGLE-2006-BLG-109Lb+c is a scaled-down version of Jupiter-Saturn, with the mass of the lensing star  $M_* = 0.5 M_\odot$ , the inner planet  $0.73 M_{\text{jup}}$  and  $r = 2.3 \text{ AU}$  ( $\sim 0.5 M_{\text{jup}}, 0.57 r_{\text{jup}}$ ), and the outer planet  $0.27 M_{\text{jup}}, r = 4.5 \text{ AU}$  ( $\sim 0.5 M_{\text{sat}}, 0.57 r_{\text{sat}}$ ). Models showed the source star first to have passed through folds and close to cusps of the resonant caustic of the smallest of the planets (1-4 in the left panel, detailed in the four first panels to the right) and then finally close to a cusp of the larger planet (5 in left panel and last panel to the right). Because of the long caustic passage time, the caustic topology changed during the passage, adding information which made it possible to estimate the eccentricity and inclination of the “Saturn-planet” to  $e = 0.15$  and  $i = 64^\circ$ . Middle panel shows the changing resonant caustic and the source path. Gray dotted and dash-dotted lines show what the models would have looked like without inclusion of the effect of parallax and finite source (based on data in Gaudi et al. 2008)

using adaptive optics at large telescopes or taking images with small-pixel cameras in space, such as HST or JWST. A much less expensive solution can be obtained by using lucky imaging technology on medium-sized telescopes, which at the same time makes it possible to perform long time series and time-consuming surveys, which in general will not be possible at large facilities or expensive space telescopes. Modern EMCCD detectors (e.g., Skottfelt et al. 2015) can obtain up to 40 images per second with basically no readout interruption and readout noise. This speed will beat the atmospheric turbulence and can in this way reach diffraction-limited spatial resolution images in fields of sizes typically a square arc minute. More advanced CMOS chips can be butted and therefore in principle be both widefield (e.g.,  $1^\circ \times 1^\circ$ ) and near diffraction limited in spatial resolution (Mackay et al. 2017).

Typical resolution by a standard CCD detector at a 2 m class telescope will make it possible to resolve source stars down to  $10 R_\odot$  in the Galactic center, which has allowed detection down to Earth-mass exoplanets orbiting M-dwarf lensing stars. Simulations of fields toward the Galactic center indicate that improving the resolution by a factor of  $\sim 3$  will make it possible to reach the main sequence at  $R_* \sim 1 R_\odot$  in the crowded fields around the Galactic center, making it possible to detect lensing objects as small as the mass of the Moon according to Eq. 5. Since the higher cadence of sufficient number of source stars in crowded fields are possible with widefield surveys, a CMOS-based widefield lucky imaging camera on a medium-sized telescope would be able to reduce the reachable host star mass, as well as the exoplanet mass, giving information about a wider range of host star populations, including substellar hosts such as brown dwarfs, but also such hypothetical populations as free-floating Jupiter-mass planets and their possible populations of Galilean mass, or larger, moons (Liebig and Wambsganss 2010; Hwang et al. 2017).

---

## The Source Star Atmosphere

The microlensing phenomenon is a combined event involving all potential objects within the small angular region of the Einstein radius of the lens. In most cases this will be only one lensing star and one source star, but it can involve a multi-lens object (of which one or more could be exoplanets) and/or a multisource object (of which one or more could be exoplanets). The level of complexity in the analysis of the lensing event increases rapidly with the number of objects involved. Only two two-planet lensing systems have been identified so far. Binary lens stars as well as binary source stars have been modelled, but no source star exoplanets have been identified. It is indicative of the complexity, relative youth and large potential of the microlensing technique that, for example, the four-component lensing event OGLE-2010-BLG-117, discovered in 2010, was only convincingly modelled as recent as 2018 (Bennett et al. 2018). The event was found to involve a binary source star lensed by a scaled-down Jupiter-analog system of a lensing star of half a solar mass orbited by a half Jupiter-mass exoplanet in an orbit half the size of Jupiter's.

While such complex analyses in the future will be able to give important statistical information about the source star population, the most straightforward benefit from the lensing in studying the source stars is by just taking advantage of the amplification of their brightness and in this way using the lens as if it was effectively “increasing the diameter of the telescope.” The studies of the Bulge stars have traditionally been biased toward the intrinsically very brightest giants, for obvious observational reasons. As for the lens star population, the source star population in the lensing events offers the advantage of a less biased sample, because nature itself selects the source stars randomly, at the same time as making them more accessible by our telescopes. The first few stars that were studied during lensing events turned out to be surprisingly metal rich compared to what is usually believed about the Bulge star population. This includes both the Bulge dwarf star OGLE-2006-BLG-265S (“S” for the “source star” as opposed to “L” for the lens star component in the event) observed at a magnification of 135 (Johnson et al. 2007) and the Bulge dwarf OGLE-2007-BLG-349S (Cohen 2008) observed at a magnification of 400. In both events high-quality spectra were obtained from the 10 m Keck telescope during the high magnification, increasing the “effective telescope diameter” to 120 m and 200 m, respectively, and hence increasing the sensitivity beyond what even the giant ELT telescope will be able to obtain. The latest summary of observations of the source component in 90 microlensing events observed near maximum amplification points at a very broad and complex metallicity and age distribution of the source stars, with a high fraction high metallicity stars (Bensby et al. 2017).

Another peculiar advantage can be achieved if one is able to obtain source star spectra during the caustic crossing. As described above, the caustic crossings give rise to very abrupt (i.e., “caustic”) changes in the magnification of the source over short time scales. If the source star has a large angular diameter and/or a low angular velocity relative to the lens, then spectra taken with few minutes or hours difference during the crossing will reflect different relative magnification of different parts of the source star atmosphere. Such was the case with, for example, the limb-darkening monitoring visible for OGLE-2004-BLG-482 (Zub et al. 2011) or the change in the H $\alpha$  line observed during the caustic passage in OGLE-2002-BLG-069 (Cassan et al. 2004) shown in Fig. 3, and one could also envision changing spectra due to differential magnification of large star spots and any other otherwise unresolvable spatial structures.

---

## Summary

Microlensing has proven to be able to characterize the population of exoplanets in terrestrial and larger-sized orbits, discovering planets as small as one Earth mass and giving statistical information about the mass distribution down to about five Earth-mass planets (Gould et al. 2010; Cassan et al. 2012). Present instrumentation under development for medium-sized telescopes will make it possible to extend the detections down to Moon-mass objects and to free-floating planets too (Mackay et al. 2017). The analysis of the light curves associated with the discovery of

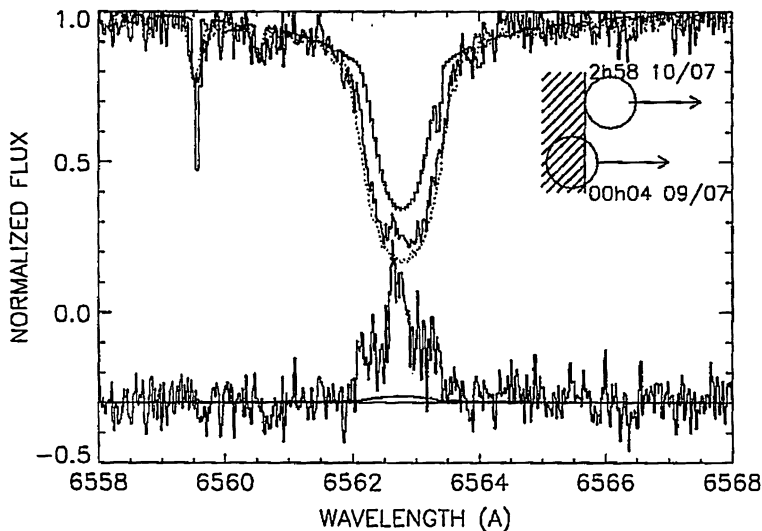


**Fig. 3** Two observations of the  $H\alpha$  spectral line of OGLE-2002-BLG-069S obtained during the passage out of the caustic region of the lens in 2002. The first spectrum (with the line being the weakest of the two exposures) was obtained at UT 00:04 on July 9, while the stronger line (with a blue-shifted emission core) is from the spectrum obtained at 02:58 on July 10. The lower part of the plot shows the difference between the two lines. On July 10, the chromosphere is strongly magnified relative to the photosphere, and one sees a blue-shifted chromospheric  $H\alpha$  emission line revealing a mass flow through the atmosphere with a velocity of  $\sim 10$  km/s. The insets in the upper right corner show the modeled position of the source star relative the caustic (shaded region) during the two exposures. (adapted from Cassan et al. 2004)

microlensing exoplanets is a multiparameter fit that gives the best fit solution to the exoplanets as well as their host stars. In this way the analyses of microlensing exoplanets simultaneously provide information about the host stars, potentially including such information as the existence of associated circumstellar and debris disks, and in particular the method provides unbiased information about which types of host stars are orbited by which type of exoplanets. By obtaining simultaneous observations from ground and space, one can obtain absolute mass determination of the host star population. Typically the source and lens stars move with a relative speed of about 1 mas per month, which will make them separable in high-resolution images  $\sim 10$  years after the lensing event has taken place. At that time, more detailed information about the host stars can be obtained and hence putting new constraints on the star-planet solution. The lensing event can also be used to obtain unprecedented information about the detailed structure of the source star atmosphere and to analyze otherwise unreachable faint populations of objects, such as the dwarf star population in the Galactic Bulge. With the expected number of microlensing exoplanets being counted in thousands within a few years of new instrumental development, microlensing is therefore the only known method to give us statistically unbiased information about the distribution of various types of

exoplanetary systems as function of host star type, including stars all the way down to the brown dwarf regime. Since microlensing is sensitive to host stars over a large distance interval, the technique is also well prepared to reveal information about the distribution of exoplanets and their host star populations as function of Galactic distance, as well as, at least in principle, through to the nearest other galaxies too.

---

## References

- Bennett DP et al (2018) *AJ* 155:141  
Bensby T, Feltzing S, Gould A et al (2017) *A&A* 605:89  
Bozza V et al (2012) *MNRAS* 424:902  
Cassan A et al (2004) *A&A* 419:L1  
Cassan A et al (2012) *Nature* 481:167  
Cohen J et al (2008) *ApJ* 682:1029  
Dai X, Guerras E (2018) *ApJL* 853:L27  
Dominik M et al (2007) *MNRAS* 380:792  
Einstein A (1936) *Science* 84:506  
Gaudi et al (2008) *Science* 319:927  
Gould A, Loeb A (1992) *ApJ* 396:104  
Gould A et al (2009) *ApJ* 698:147  
Gould A et al (2010) *ApJ* 720:1073  
Henderson CB et al (2016) *PASP* 128:124401  
Høg E, Novikov ID, Polnarev AG (1995) *A&A* 294:287  
Hundertmark M, Hessman FV, Dreizler S (2009) *A&A* 500:929  
Hwang KH, Udalski A, Bond IA et al (2017, submitted) *AJ*. arXiv1711.09651  
Ingrosso G, Novati S, Calchi, de Paolis F et al (2009) *MNRAS* 399:219  
Johnson JA et al (2007) *ApJ* 655:L33  
Liebig C, Wambergans J (2010) *A&A* 520:68  
Mackay C et al (2017) Submitted arXiv1709.00244  
Mao S, Paczynski B (1991) *ApJ* 374:L37  
Mróz P et al (2017) *Nature* 548:183  
Paczynski B (1998) *ApJ* 494:L23  
Refsdal S (1964) *MNRAS* 128:295  
Ryu YH et al (2018) *AJ* 155:40  
Sajadian S, Rahvar S (2015) *MNRAS* 454:4429  
Skottfelt J et al (2015) *A&A* 573:103  
Street RA et al (2016) *ApJ* 819:93  
Shvartzvald Y, Maoz D, Udalski A et al (2016a) *MNRAS* 457:4089  
Shvartzvald Y et al (2016b) *ApJ* 831:183  
Udalski A et al (2018) *Acta Astronomica*, 68:1  
Yee J et al (2015) *ApJ* 802:76  
Zub M et al (2011) *A&A* 525:A15